

This article was downloaded by:

On: 22 January 2011

Access details: *Access Details: Free Access*

Publisher *Taylor & Francis*

Informa Ltd Registered in England and Wales Registered Number: 1072954 Registered office: Mortimer House, 37-41 Mortimer Street, London W1T 3JH, UK



The Journal of Adhesion

Publication details, including instructions for authors and subscription information:

<http://www.informaworld.com/smpp/title~content=t713453635>

Stresses in an Adhesive Bond at an Adhesive/Adherend Interface Under Load

Paul Predecki^a; Charles S. Barrett^a; Alan B. Lankford^d; D. Gutierrez-lemini^b

^a University of Denver, Denver, CO ^b United Technologies Corp., Sunnyvale, CA, U.S.A.

To cite this Article Predecki, Paul , Barrett, Charles S. , Lankford, Alan B. and Gutierrez-lemini, D.(1986) 'Stresses in an Adhesive Bond at an Adhesive/Adherend Interface Under Load', The Journal of Adhesion, 19: 3, 207 – 218

To link to this Article: DOI: 10.1080/00218468608071224

URL: <http://dx.doi.org/10.1080/00218468608071224>

PLEASE SCROLL DOWN FOR ARTICLE

Full terms and conditions of use: <http://www.informaworld.com/terms-and-conditions-of-access.pdf>

This article may be used for research, teaching and private study purposes. Any substantial or systematic reproduction, re-distribution, re-selling, loan or sub-licensing, systematic supply or distribution in any form to anyone is expressly forbidden.

The publisher does not give any warranty express or implied or make any representation that the contents will be complete or accurate or up to date. The accuracy of any instructions, formulae and drug doses should be independently verified with primary sources. The publisher shall not be liable for any loss, actions, claims, proceedings, demand or costs or damages whatsoever or howsoever caused arising directly or indirectly in connection with or arising out of the use of this material.

J. Adhesion, 1986, Vol. 19, pp. 207–218
0021-8464/86/1904-0207 \$18.50/0
© 1986 Gordon and Breach Science Publishers, Inc.
Printed in the United Kingdom

Stresses in an Adhesive Bond at an Adhesive/Adherend Interface Under Load

PAUL PREDECKI, CHARLES S. BARRETT and ALAN B. LANKFORD

University of Denver, Denver, CO 80208

D. GUTIERREZ-LEMINI

United Technologies Corp., Sunnyvale, CA 94086, U.S.A.

(Received January 25, 1985; in final form August 26, 1985)

Triaxial stresses were determined by X-ray diffraction immediately adjacent to the adhesive/adherend interface of a single lap adhesive bond while under a tensile load. One adherend was a Be strip that was relatively transparent to the X-rays; the X-ray beam passed through this and the layer of FM-73M adhesive to diffract from the surface of the other adherend which was of 6061 aluminium alloy suitably annealed. The thicknesses of the Be and Al were made such that their stiffness in tension was matched.

Measured stresses were compared with stresses calculated using the Texgap-2D finite element code for a nominally identical joint and at a depth of 0.033 mm into the Al adherend which coincided with the average depth from which the X-ray data were obtained. The comparison showed a general agreement in trends and magnitudes except at the extremities of the bond. In particular the measured peel stress was found to be substantially larger at one extremity than the calculated peel stress. Possible causes of the discrepancies are discussed.

KEY WORDS Adhesive/adherend interface; Adhesive bond; Finite element method; Lap specimen; Stress distribution; X-ray diffraction.

INTRODUCTION

By the use of X-ray diffraction and appropriate adherends it has become possible to measure, we believe for the first time, the

triaxial stresses existing immediately adjacent to the adhesive/adherend interface of a single lap joint. Both the residual stresses introduced by cooling the adhesive from the curing temperature and the stresses existing when the cured joint is loaded in tension can be measured.¹ Measurements in these two conditions together with measurements of an adherend free from any residual, curing and loading stresses permit determination of the stress components that are due to loading only. These can then be compared with stresses calculated for the same joint by finite element methods. The importance of stresses at the adhesive/adherend interface is that bond failures frequently originate here. The difficulties of access to this interface are overcome by making one of the adherends of beryllium and the other of aluminium alloy. The X-rays (CuK α radiation) penetrate the Be and the adhesive and diffract from the Al before escaping to a detector system. The X-ray penetration depth into the Al (95% absorption) with normal incidence is 0.11 mm, so that most of the diffraction information is coming from Al grains at or near the Al/adhesive interface.

SAMPLE PREPARATION

For the present experiments, single lap joints were made with dimensions shown in Figure 1. The Al alloy selected was 6061 in the T4 condition (solution treated and quenched). Solution treatment reduced the yield strength to ~ 193 MPa (28 ksi) but substantially improved the diffraction peak sharpness. The Be was made 1/4 the thickness of the Al since the Young's modulus of Be is 4 times that of Al. The joint was therefore approximately of balanced stiffness in tension but not in bending. The adhesive used was FM-73M[†] (rubber modified epoxy with polyester mat), a common structural sheet adhesive.

Specimens of the type shown in Figure 1 were fabricated using a brass jig which maintained alignment and a uniform adhesive thickness (± 0.013 mm). If the standard bonding procedure for the FM-73M were followed, the adhesive layer would contain numerous bubbles as shown in Figure 2(a). The following modified procedure

[†] American Cyanamid Co., Havre de Grace, MD.

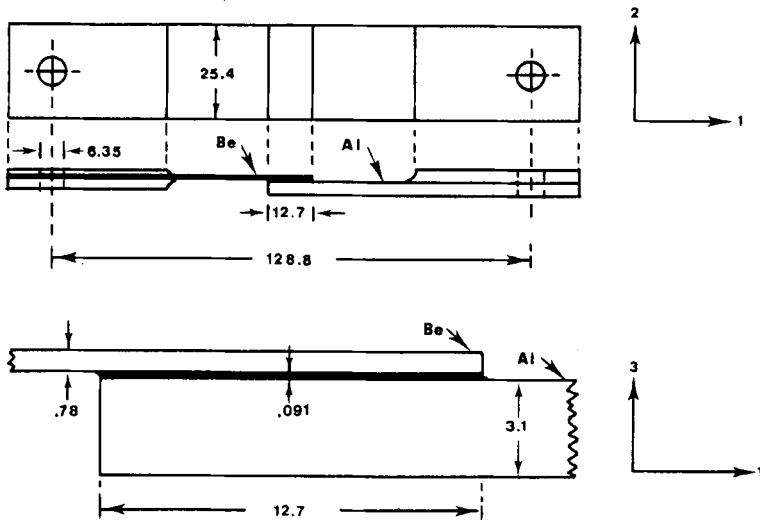


FIGURE 1 Dimensions in mm of the single lap joint specimen (ARO-23) used for stress determination. Tab thicknesses at the ends were made such that the central plane of the section at each clevis pin was coplanar with the plane of the adhesive layer at the center of the specimen.

eliminated the bubbles as is evident in Figure 2(b). Both adherends were degreased in trichloroethylene. The Al adherend was dry-abraded with 320 grit SiC to remove all traces of rolling and heat treating scale. The Be adherend was etched 1 to 2 min in the following etchant: 2% HF + 2% HNO₃ + 2% H₂SO₄, with the balance deionized H₂O,[†] which removed about 0.025 mm Be/min, followed by rinsing, swabbing in deionized water and drying. Both adherends were primed by applying a thin dip coat of BR 127 primer (American Cyanamid Co.), air drying and curing 30 min at 120°C. One layer of 0.010" thick FM-73M (stored in freezer) was placed on the Al adherend in the brass jig preheated to 70°C. The jig was placed in a liquid N₂-trapped vacuum oven at 70–80°C for ~10 min while most of the volatiles bubbled out of the adhesive. The vacuum was then released, the two adherends joined together, clamped in the alignment jig and cured at 120–125°C for 1 hr in air.

[†] Courtesy of Brush-Wellman Beryllium Co.

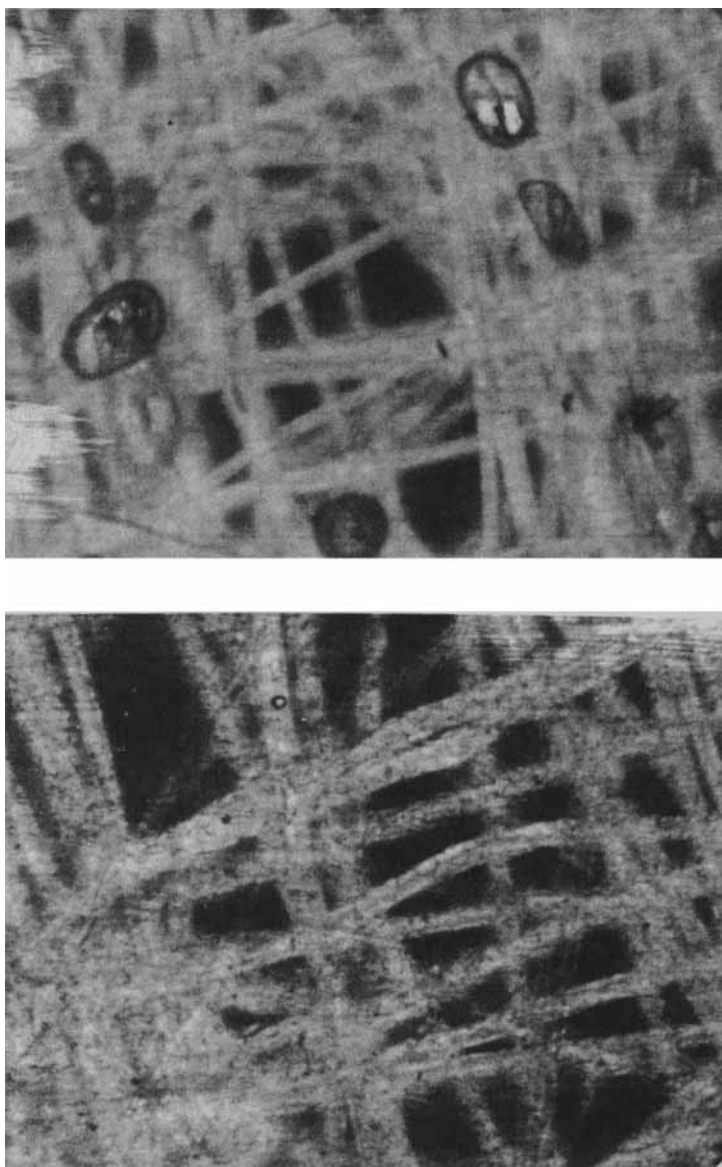


FIGURE 2 FM-73M cured adhesive layers recovered from single lap joints by dissolving away the adherends in NaOH solution after bonding, (a) standard bonding procedure, (b) modified procedure developed for this project. Optical micrograph, 50 × magnification.

To prevent bubble formation in the bond it was important to release the vacuum before bonding and to do the curing at ambient pressure, not in vacuum.

After cooling to room temperature, the excess adhesive spew was carefully machined off and end tabs for the clevis grips were attached with Hysol EA 9309 epoxy adhesive.

MEASUREMENTS

The methods used for the X-ray strain measurements and the stress calculations are described in detail elsewhere.¹ Briefly, the sample was placed between clevis type grips in a small, manually operated tensile frame with load cell. The frame was mounted on the horizontal goniometer table of a Siemens diffractometer in such a manner that the diffractometer rotation axis was in the 2 direction (vertical) and in the plane of the Al/adhesive interface. Incident and diffracted beams were in the 1, 3 plane and load was applied in the 1 direction. Diffracted beams were also measured with the specimen turned with the 1 direction vertical, but not loaded. The 333 + 511 reflection from Al at $\sim 162.5^\circ 2\theta$ with $\text{CuK}\alpha_1$ radiation was used for all measurements. Diffracted beams were passed through a graphite monochromator before entering a scintillation counter.

The direction of strain measurement (the bisector of the angle between the incident and diffracted beams) was specified in the usual way² using the angles ϕ and ψ where ψ indicates the tilt of the measurement direction from the 3 direction and ϕ the azimuthal position projected onto the 1, 2 plane. Measurements of diffracted peak position were made on bonded specimens along the center line in the 1 direction at the following angles: $\phi = 0$, $\psi = 0$, ± 45 and $\phi = 90$, $\psi = \pm 45$. Near the ends of the bond, the ψ angles were restricted to avoid passing the beam through the ends of the bond. Irradiated areas on the sample were as follows: 1.4 mm wide (in the 1 direction) \times 7 mm high (in the 2 direction) for $\phi = \psi = 0$ and 2.8 mm wide \times 1.6 mm high for $\phi = 90$, $\psi = 0$. The beam width was reduced to 0.56 mm to improve spatial resolution near the ends of the bond for $\phi = 0$.

Measurements were also made on blank adherend samples

prepared identically to the bonded adherend to obtain "stress free" values of the peak positions at all ϕ and ψ settings used. All peak positions were determined by 5-point step scanning and least-squares fitting of a parabola to these points. It was found advisable to rock all specimens $\pm 1^\circ$ during exposure to increase the number of grains diffracting (the Al grain size was ASTM #6). Small corrections were made to ψ for rocking and for slight rotation of the joint when load was applied. Peak positions were corrected for Lorentz-polarization and absorption.

RESULTS AND DISCUSSION

The strains, $\epsilon_{\phi\psi}$, whether residual (due to curing) or residual + applied, were determined from

$$\epsilon_{\phi\psi} = \frac{\sin \theta_{\phi\psi}^\circ - 1}{\sin \theta_{\phi\psi}} \quad (1)$$

where $\theta_{\phi\psi}$ is the Bragg angle in the as-cured or as-cured + loaded condition and $\theta_{\phi\psi}^\circ$ is the corresponding angle in the "stress free" condition. These strains were then expressed in terms of strains in the 1, 2, 3 (specimens) system of axes using the transformation equations as follows:

$$\begin{aligned} \epsilon_{0,\psi} &= \epsilon_{11} \sin^2 \psi + \epsilon_{13} \sin 2\psi + \epsilon_{33} \cos^2 \psi \\ \epsilon_{90,\psi} &= \epsilon_{22} \sin^2 \psi + \epsilon_{23} \sin 2\psi + \epsilon_{33} \cos^2 \psi \end{aligned} \quad (2)$$

Eqns (2) were solved for ϵ_{11} , ϵ_{22} , ϵ_{33} , ϵ_{13} and ϵ_{23} using the corrected ψ values employed in the measurements. It was assumed that ϵ_{12} (as cured) was zero as expected from symmetry and that ϵ_{22} (cured + load applied) = ϵ_{22} (as cured), *i.e.* that ϵ_{22} remained constant with applied load, an assumption made by most analytical and finite element treatments of single lap joints.³⁻⁶ The latter assumption made it unnecessary to make measurements under applied load in the $\phi = 90$ orientation.

From these strains, the corresponding normal and shear stresses were determined from isotropic elasticity using the equations:²

$$\begin{aligned} \sigma_{ij} &= \epsilon_{ij} / \left(\frac{1}{2} S_2\right) && \text{(shear)} \\ \sigma_{ii} &= [\epsilon_{ii} / \left(\frac{1}{2} S_2\right)] - KE && \text{(normal)} \end{aligned} \quad (3)$$

where $K = S_1[\frac{1}{2}S_2(\frac{1}{2}S_2 + 3S_1)]^{-1}$ and $E = \epsilon_{11} + \epsilon_{22} + \epsilon_{33}$. The X-ray elastic constants $\frac{1}{2}S_2$ and S_1 were determined in a separate experiment from the slope and intercept of a $\text{Sin}^2 \psi$ vs ϵ_{33} plot in the usual manner. The values obtained from a tensile specimen of the Al adherend material were: $\frac{1}{2}S_2 = 1.91 \times 10^{-5} \text{ MPa}^{-1}$ ($131.8 \times 10^{-9} \text{ psi}^{-1}$) and $S_1 = -5.15 \times 10^{-6} \text{ MPa}$ ($-35.5 \times 10^{-9} \text{ psi}^{-1}$).

The residual stresses thus obtained for the as-cured condition were then subtracted from those for the cured plus loaded condition (interpolating where necessary) to obtain the net stresses due to the applied load of 2669 N (600 lbs). These net stresses from the X-ray measurements are shown in Figures 3-6 and are compared with the stresses calculated by the finite element method for a nominally identical joint loaded in the same manner and with the same applied load.

Errors in the measured stresses of Figures 3-6 were estimated by randomly introducing the average standard deviation of the peak

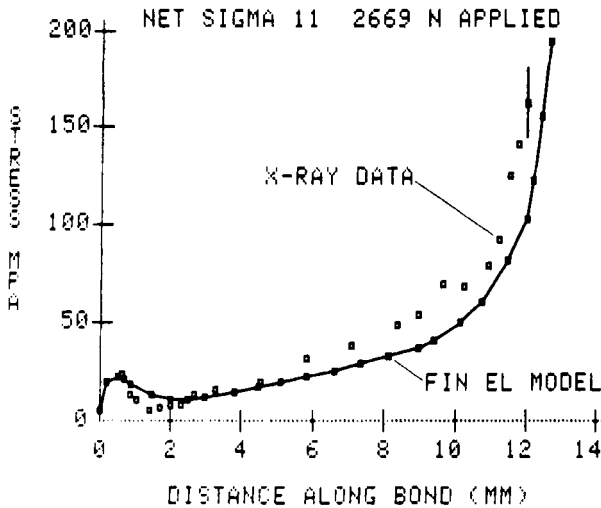


FIGURE 3 Comparison of normal stress, σ_{11} , measured by X-ray diffraction and calculated by the Texgap-2D finite element program (fin. el. model) along the Be/FM-73M/Al (6061-T4) single lap joint of Figure 1. Here and in Figures 4, 5 and 6; the measured and calculated stresses are in the Al adherend at a depth of 0.033 mm from the Al/adhesive interface; the edges of the Al and Be adherends are at 0 and 12.7 mm, respectively.

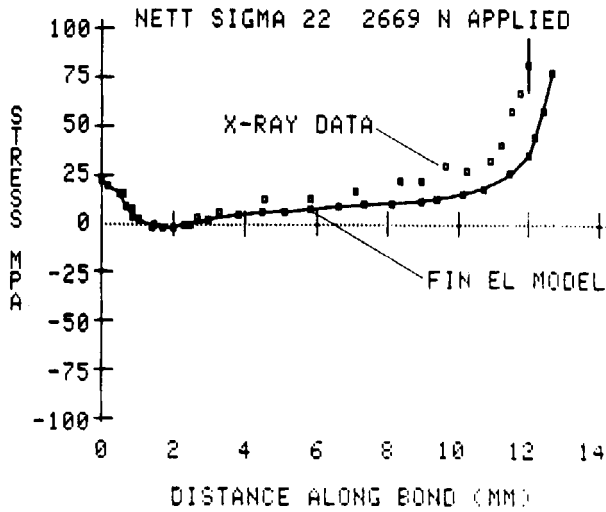


FIGURE 4 Comparison of normal stress σ_{22} measured by X-ray diffraction and calculated by the Texgap-2D program along the Be/FM-73M/Al (6061-T6) single lap joint of Figure 1.

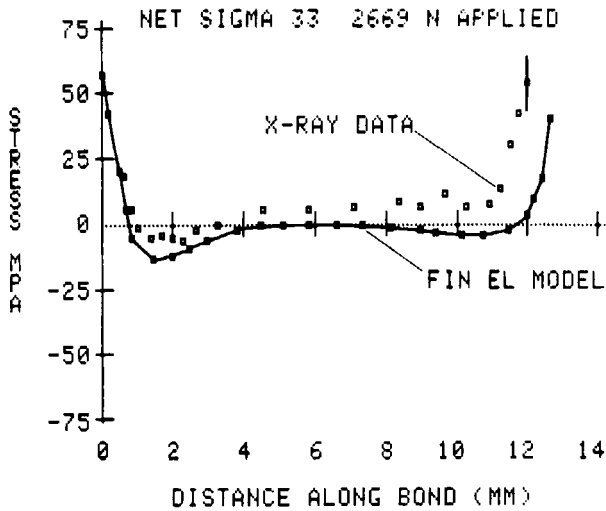


FIGURE 5 Comparison of normal peel stress σ_{33} measured by X-ray diffraction and calculated by the Texgap-2D program along the Be/FM-73M/Al (6061-T6) single lap joint of Figure 1.

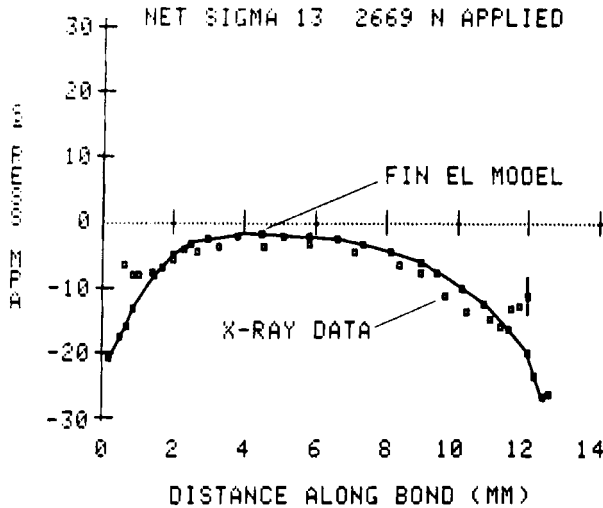


FIGURE 6 Comparison of shear stress σ_{13} measured by X-ray diffraction and calculated by the Texgap-2D program along the Be/Fm-73M/Al (6061-T6) single lap joint of Figure 1.

position ($\Delta 2\theta = \pm 0.01^\circ$) into the 2θ values used in the stress calculation. The standard deviations of the stresses were obtained from averaging 7 such random introductions; they varied from 1 to 27 MPa (0.14 to 3.8 ksi), generally increasing with stress. Errors were necessarily larger near the extremities of the bond where a narrower X-ray beam was used to improve spatial resolution and where the ψ range was restricted.

Since X-rays are absorbed exponentially, the exponentially weighted average penetration depth for $\text{CuK}\alpha_1$ radiation in Al for the ψ angles used was calculated and found to be 0.033 mm. Accordingly, the finite element stresses shown in Figures 3–6 are for positions at this depth within the Al adherend. Finite element calculations were also made at the Al/adhesive interface. These were virtually identical with those 0.033 mm below the interface except for σ_{13} , for which the interface values were 10–15% more negative than the 0.033 mm values, but only at the extremities of the bond.

The program used was Texgap-2D which is a finite element code designed for analysis of two-dimensional static problems of linear

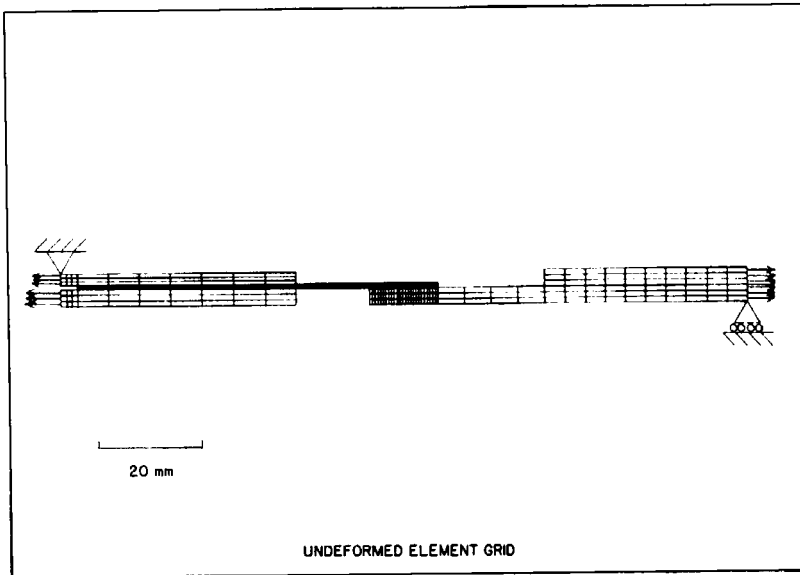


FIGURE 7 Finite element model of the sample. Dimensions and materials are nominally the same as the X-ray sample, Figure 1.

elasticity. The finite element model of the sample used is shown in Figure 7 and has the same dimensions and materials as the joint used for the X-ray work. The elastic constants used were: 27.6×10^4 , 6.9×10^4 and 0.1929×10^4 respectively for the Young's moduli of Be, Al and FM-73M (40 , 10 and 0.28×10^6 psi) and 0.33 , 0.33 and 0.32 respectively for the Poisson's ratios. The model was assembled with the quadratic-displacement isoparametric quadrilateral available in Texgap-2D. The analysis performed corresponded to the plane strain condition. Three layers of elements were used through the thickness of the adhesive and initially no attempt was made to capture the stress singularities present at the reentrant corners between the adherends and the adhesive layers. In a subsequent calculation, the number of elements near the corner where the Be adherend ended was increased from 13 to 224. This resulted in increases of 7.5%, 9.9% and 29% in σ_{11} , σ_{22} and σ_{33} , respectively, at the extreme edge of the bond, while σ_{13} became more negative by 43% here also. The fine mesh values are the ones

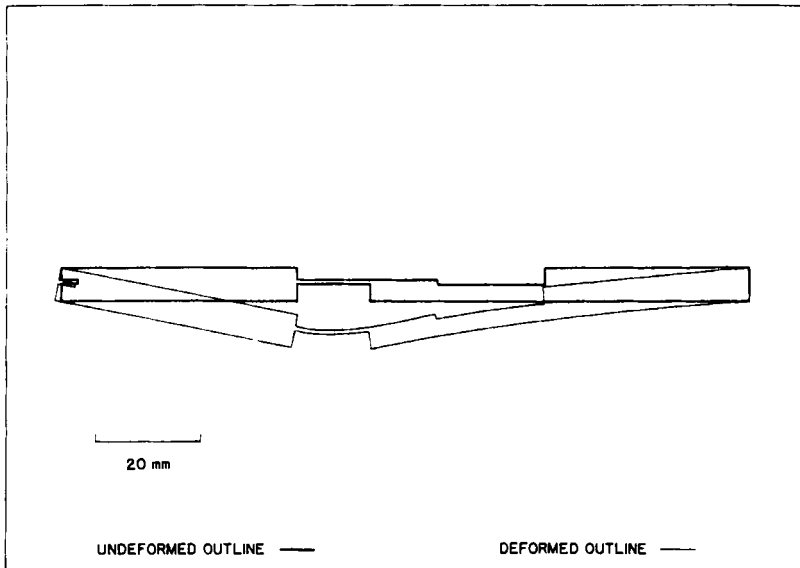


FIGURE 8 Computer sketch of the geometry of the finite element sample with and without a static load of 2669 N (600 lbs) applied. Distortion at load is much amplified.

used in Figures 3–6 for the last 0.5 mm of the bond from 12.2 to 12.7 mm. Figure 8 is a computer sketch comparing the geometry of the test sample with and without a static load of 2669 N (600 lbs) applied.

Figures 3–5 show that there is general agreement in both trends and magnitudes between calculated and measured stresses. There is an increasing discrepancy between the two as the end of the Be adherend, (end B), is approached which is not fully accounted for by use of a finer finite element mesh size at this end. In particular, the measured peel stress here is substantially larger than that calculated. The discrepancy looks like a sample displacement error of about 1 mm in the 1 direction in the X-ray measurements; however, the beam width here was 0.56 mm, so this displacement error is probably ≤ 0.28 mm. Another displacement error arises because the stress distribution in the irradiated area increases more rapidly than linearly as end B is approached (Figures 3–5). Therefore, the mean measured stress in the irradiated area

(0.56 mm width) is weighted to a greater extent by the portion of this area closest to the end B than would be expected in the linear case.

Alternate possibilities that may account for these discrepancies and those in σ_{13} at the extremities of the bond (Figure 6) are (1) that a small crack or debond in fact exists at end B which effectively moves the stress distributions to the left about 1 mm in Figures 3–5. (2) The adhesive near end B is thicker than the 0.091 mm assumed in the calculation because of rounding of the edges of the Be adherend in the etching step. (3) The structure and elastic constants of the adhesive may be different at the extremities of the bond because the ratio of adhesive to matte is likely to be different at the bond extremities than the bond interior as a result of the pressure gradient during bond fabrication. To explore some of these possibilities, specimens containing intentional short debonds at end B will be prepared for X-ray measurement and finite element calculation.

Acknowledgement

This work was supported by the U.S. Army Research Office on Grant No. DAAG29-81-0150. We are grateful to W. B. Jones of Texas Tech University and L. J. Hart-Smith of Douglas Aircraft Co. for several valuable discussions, and to Richard Miller for help with specimen preparation.

References

1. P. Predecki and C. S. Barrett, *Advances in X-ray Analysis* **27**, 251 (1984).
2. See for example, J. B. Cohen, H. Dolle and M. R. James, Stress Analysis from Powder Diffraction Patterns, in *NBS Special Pub. 567: Accuracy in Powder Diffraction*, S. Block and C. R. Hubbard, Eds. (NBS, Washington, DC, 1980), pp. 453–477.
3. R. D. Adams and N. A. Peppiatt, *J. of Strain Analysis* **9**, 185 (1974).
4. *Viscoelastic Stress Analysis Including Moisture Diffusion for Adhesively Bonded Joints*, J. Romanko, P. I., MRL Report FZM-6838, General Dynamics, Fort Worth (1980).
5. W. J. Stronge and O. E. R. Heimdahl, *Stress in Single Lap Joints of Dissimilar Materials*, Naval Weapons Center, China Lake, Report NWC TP 6242 (1981).
6. E. C. Francis, *et al.*, *Time Dependent Fracture in Adhesive Bonded Joints*, Interim Report for 24 Sept. 1981 to 24 April, 1982, Chemical Systems Division, prepared for Air Force Wright Aeronautical Laboratory, Wright-Patterson Air Force Base. CSD2769-IR-01.